Open Access Research Journal of
Life Sciences
Journals home page: https://oarjpublication/journals/oarjls/
ISSN: 2783-025X (Online)

OARJ OPEN ACCESS RESEARCH JOURNALS

(RESEARCH ARTICLE)

Check for updates

Dual morphometric and microcellular spatial distribution analysis during zone-specific callogenesis in *Fouquieria splendens*

Jorge Adrián Paz-Delgado [1], Carlos Fabián Vargas-Mendoza [2] and Angélica Rodríguez-Dorantes [1,*]

[1] *Plant Physiology Laboratory, Botany Department, School of National Biological Sciences, National Polytechnic Institute, México City 11340, México.*
[2] *Variation and Evolution Laboratory, Zoology Department, School of National Biological Sciences, National Polytechnic Institute, México City 11340, México.*

Open Access Research Journal of Life Sciences, 2026, 12(01), 018–027

Publication history: Received on 30 June 2026; revised on 04 August 2026; accepted on 06 August 2026

Article DOI: https://doi.org/10.53022/oarjls.2026.12.1.0027

Abstract

Plant growth, development, and physiology had a complex process across scales from molecular, cellular, tissue, and whole organism. Particularly, the plant *in vitro* studies have the attention on individual aspects of plant development. Mathematical and computational analysis are powerful tools that allow the integration of experimental data associated to *in vitro* mophogenesis of plants by image processing techniques. This work characterized the morphometric features of selected development zones of *Fouquieria splendens* callus by the analysis of scanning electron microscopy images and the spatial distribution of cells to describe the length and position of them on callogenesis process. Principal Component Analysis (PCA) successfully discriminated the developmental zones, accounting for 73.34% of the total explained variance and revealing that callogenesis is governed by discrete, predictable morphogenetic transitions with a coordinated and hyper-regular microcellular dispersion across all evaluated regions that effectively mitigate chaotic or disordered growth. Also, macrostructural descriptors showed homeostatic stabilizing agents that restore tissue density homogeneity. Finally, the fixed geometric canalization observed in roundness and aspect ratio parameters confirms that mechanical and structural stimuli strictly regulate cellular shape prior to massive volumetric cell expansion processes showing together the *in vitro* cellular mass development in this xerophytic species.

Keywords: Fouquieriaceae, Callus Culture; Scanning Electron Microscopy; Morphometrics

1 Introduction

To analyze and obtain numerical data from images, the software ImageJ, can be employed in biological sciences and environmental sciences as in others [1,2]. Particularly, it has been employed by some authors [3-9] to quantify and compare cellular and subcellular components. *In vitro* mophogenesis of plants that showed slight changes in geometric features of a "callus" could be analyzed by image processing techniques that allows as Aitken-Christie et al. [10] and Ibaraki and Kenji [7] an evaluation processes that includes a visual inspection based on criteria that determine the color changes of a callus or shoot, degree of hyperhydricity and callus initiation and after their geometric analysis done by image processing techniques a better description of callus initiation allows visible *in vitro* data [10-12]. An example of it was the employ of this analysis for the automatic selection of regenerated rice calli for its acclimatization by Honda et al. [13]. Smith et al. [5] and Mansouri et al. [14] analyzed the mass of *Ajuga pyramidalis* callus employing the area obtained by view images. Particularly the studies on plant regeneration have centered on callus formation, a pluripotent cell mass triggered by wounding or exogenous hormone application [15,16], but its cellular heterogeneity in callus does not allows to understand the spatial dynamics and the cell patterns involved in the plant regeneration [17,18]. Plant callus growth presents two differential characteristics that must be considered when it is analyzed; the complex geometry of the initial callus surface and the fact that its size changes in time. Galeano et al. [19] mention that the first step for the analysis of callus growth is to choose a complex early interface of a callus as the initial reference. They made

* Corresponding author: Angélica Rodríguez-Dorantes.

this analysis by computing the center of the callus mass to know the effective growth of the callus and characterized the time evolution of it subjected to different growth conditions that can be employed to determine the basic mechanisms involved in the ontogeny of callus formation. Thus, not only some selected shape descriptors could be employed to determine the nature of the aggregated state of the cells in a growth of callus mass; it is also the employ of some ecological indices and statistics strategies that could be useful to try to analyze how them are distributed inside and make a better characterization. This work characterized the morphometric features of selected development zones of *Fouquieria splendens* callus by the analysis of scanning electron microscopy images and the spatial distribution of cells to describe the length and position of them on callogenesis process.

2 Material and methods

2.1 *Fouquieria splendens* callus culture and development

Branches of the desert plant *F. splendens*, were collected from the Botanical Garden of the Facultad de Estudios Superiores, Iztacala (FES)-UNAM and maintained in water for 15 days for the development of leaves. Leaves were surface sterilized with sodium hypochlorite solution (10%) for 90 seconds, rinsed three times in sterile distilled water and leaf explants were obtained aseptically cutting fractions of $1cm^2$. Five explants were placed separately in baby food flasks with Magenta SIGMA caps containing 25mL of Murashige and Skoog (MS) [20] ¼ salts "MSA" medium with 42.5mg/L NaH_2PO_4 + 10mg/L BAP (Bencil Amino Purine) + 1mg/L NAA (Naphthalene Acetic Acid) and supplemented with 30 g/L of sucrose and 3 g/L phytagel. Flasks were incubated at 28°C under photoperiod of 16 h light /8 h dark with a fluorescent Phillips T8 32 Watts 5000ºK lamp, finally, all the experiments were performed by 3 replicates, and growth was analyzed at 21 days.

2.2 Growth characterization of *Fouquieria splendens* callus by the analysis of SEM images

Selected fractions of *F. splendens* callus were prepared for scanning electron microscopy (SEM) for their analysis of morphological changes, according to Corona-Álvarez et al. [21] as follows: samples were cut into 4 or 5mm pieces, fixed in 2.5% glutaraldehyde for 1h at room temperature (27°C), then, washed three times in a phosphate buffer, postfixed in 1% OsO_4 for 1h at room temperature, washed and dipped into distilled water for three times. The samples were undergone a series of dehydration processes: 30 % ethanol for 10 min; 40 % ethanol for 10 min; 50 % ethanol for 10 min; 60 % ethanol for 10 min; 70 % ethanol for 10 min; 80 % ethanol for 10 min; 90 % ethanol for 10 min and finally 100 % ethanol for 10 min (three times). The material was dried in critical point dryer apparatus, mounted and sputter-coated with gold in an ion coater for 60 seconds. Finally, the samples were ready for viewing under field scanning electron microscope JEOL-JSM 5800 LV for their examination and photography. A series of callus SEM images were obtained between 40X to 45X augments, selected and adjusted to analyze by ImageJ software; at first the different and significant differentiated zones were determined in the callus images by the employ of a Pen Tablet One (WACOM) with the help of X-Journal software. These basic zones were: Differentiated Zone **(DZ)** where the incipient presence of shoots or roots characterized this zone; Cellular Aggregates Zone **(CAZ)** characterized only by the presence of cellular clusters without the extracellular matrix cover; Mechanic Damage Zone **(MDZ)** characterized by the presence of cellular damage sections by mechanical manipulation and finally the Explant Remains Zone **(ERZ)** characterized by the presence of the original explant; all of them showed in Figure 1. Is important to mention that after the SEM images were analyzed, six combined zones were recognized in the callus mass of *F. splendens* (DZ; CAZ; DZ+CAZ; DZ+MDZ; DZ+CAZ+MDZ; DZ+CAZ+MDZ+ERZ) and described by morphometric analysis.

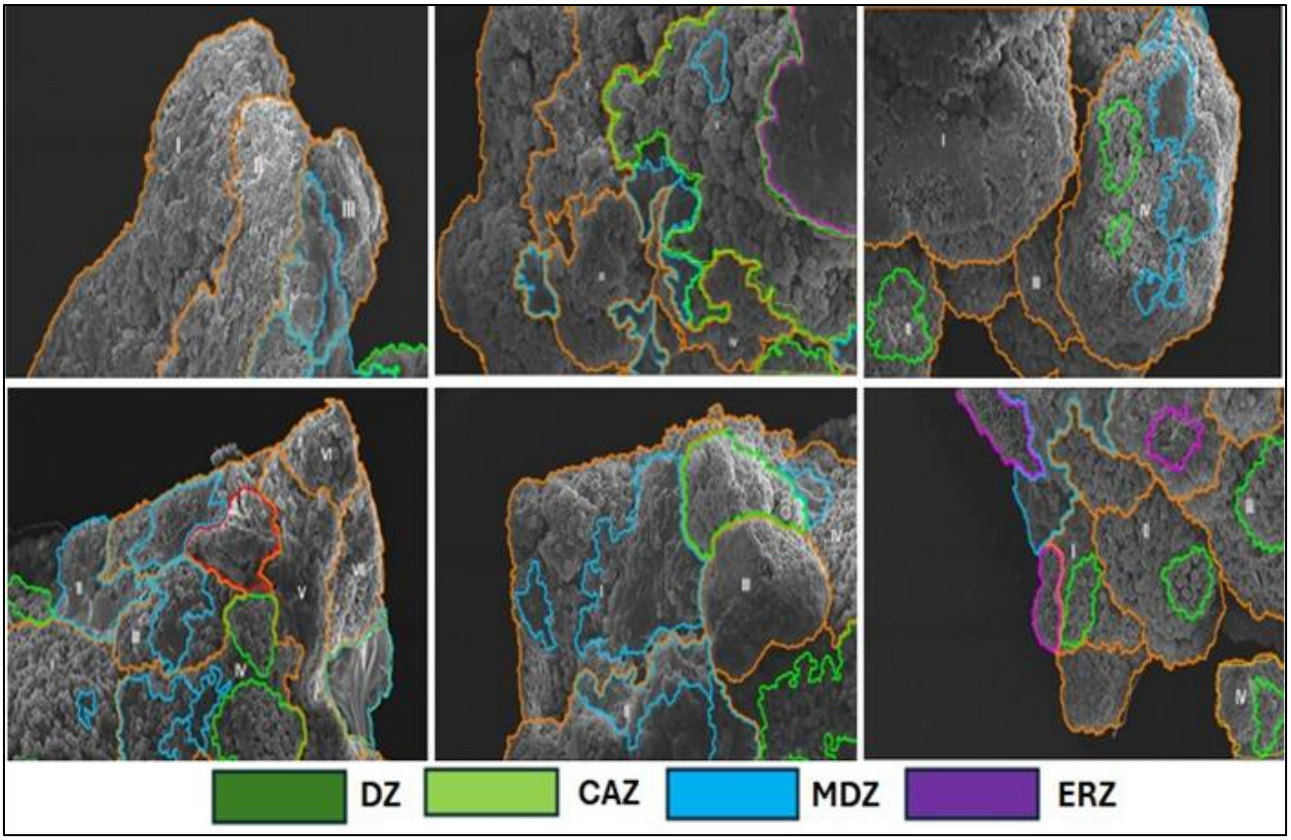

Figure 1 Basic zones determined in the SEM images of *Fouquieria splendens* callus. **DZ:** Differentiated Zone; **CAZ:** Cellular Aggregates Zone; **MDZ:** Mechanic Damage Zone and **ERZ:** Explant Remains Zone.

2.3 Analysis of *Fouquieria splendens* callus zones by segmentation and numerical data

Secondly, the morphometric analysis that includes the image segmentation; allowed the selection and characterization of cells or cell aggregates presented in the delimited zones. This was done employing the ImageJ 1.53k software and the "analyze particles command" to count and measure the objects in a selected area, scanning the image until it finds the edge of an object (Figure 2). The geometry and numerical data derived by the selected shape descriptors: total cells number; area; perimeter; roundness; Aspect Ratio (AR: the aspect ratio of the particle's fitted ellipse) and centroid (as the center point of the selection that is the average of the x and y coordinates of all of the pixels in the image selection) were exported as excel files and finally a statistical analysis of individual cells or groups of cells was done.

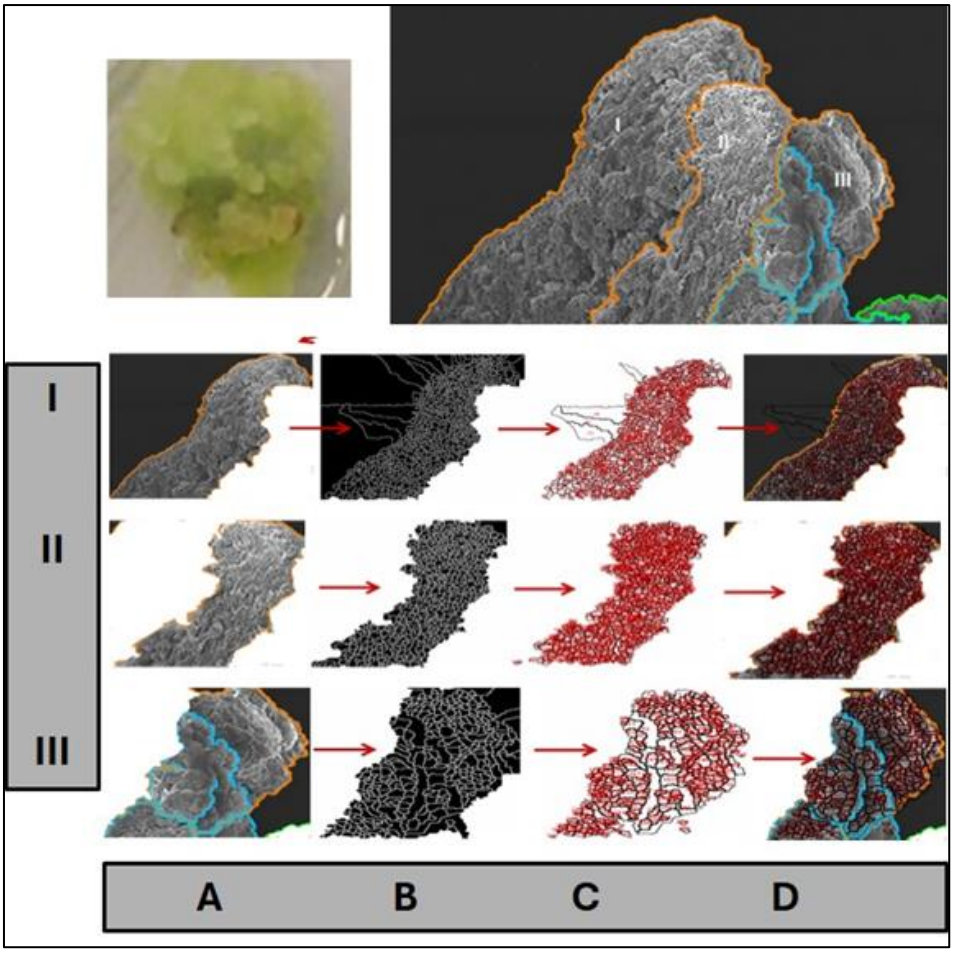

Figure 2 Morphometric analysis of the determined zones of *Fouquieria splendens* callus. **I, II and III:** are the determined zones according to the nature of the cells or cell aggregates in callus; **A, B, C and D:** are the followed processes done in the "analyze particles" of cells or cell aggregates by the employ of ImageJ software.

2.4 Morphometric and microcellular spatial distribution analysis

To achieve a rigorous characterization of spatial distribution pattern of the cellular population and development, a dual statistical approach was implemented: first, the analysis of Clark and Evans [22] Nearest Neighbor Distance Dispersion Index **(R)** that considers the observed mean distance **($đ_o$)** calculated by averaging the minimum Euclidean distances between the centroids of each adjacent pair of cells and also the expected mean distance **($đ_e$)** under a completely random distribution model, derived from the population density **(ρ)**, defined as the total number of cells of each defined zone divided by the total area of them and final index was expressed as the ratio: $đ_o/đ_e$ and demonstrated a hyper-regular distribution at the microcellular level, confirming that individual cells maintain constant and coordinated spatial separations. Secondly, the variance-to-mean ratio or dispersion index (VMR/DI) analysis corroborated that the cellular density was homogeneously distributed across the different zones of the explant, validating the global stability and uniformity of the developing mass.

2.5 Statistical analysis

All data obtained from the ImageJ software applied to *F. splendens* callus selected SEM images were analyzed at first by one-way analysis of variance, and the mean differences were compared applying a Tukey-Kramer Method using the statistics program Graph Pad Instat Ver. 2.03. The relationship between the AR and roundness of *F. splendens* cells was also analyzed by linear regression and the "x,y" centroid relationship of each callus zones was also analyzed by scatter plot. Finally, all the association and tendency of the shape descriptors data: area, perimeter, roundness and AR and the index components were analyzed by a Principal Component Analysis (PCA) measuring its correlation employing the PAST software (Paleontological Statistics Software Package) Ver. 5.3.

3 Results and discussion

3.1 General dimensions of the characterized zones of *Fouquieria splendens* callus

Table 1 shows the overall results of the metrics of the shape descriptors: **CN** (cells number); **TA** (total area); **TP** (total perimeter); **Ro** (roundness) **AR** (aspect ratio); **ρ** (cells density); $đ_o$ (observed mean distance); $đ_e$ (expected mean distance); **R** (Clark and Evans Index) and variance-to-mean ratio **(VMR/DI)**, from the characterized zones of *F. splendens* callus. The number of cells for each zone was as follows: DZ: 3,579; DZ+MDZ: 1,639; DZ+CAZ+MDZ: 1,242; DZ+CAZ: 1,214; CAZ: 881 and finally DZ+CAZ+MDZ+REZ: 743. It was clear that the callus zone with the highest total area and total perimeter values and cells number was the DZ. The rest of the zones particularly shared the values of total area between 1,009,806 to 1,555.48μm^2. Perimeter measurement values diminished according to the following order: DZ+MDZ: 177,743; DZ+CAZ+MDZ: 177,395; CAZ: 144,650; DZ+CAZ+MDZ+REZ: 97,770 and finally DZ+CAZ: 634μm. No statistical significance was determined between these shape descriptors.

Table 1 Comparative values of *Fouquieria splendens* callus metrics.

Callus Zones	CN	TA (μm^2)	TP (μm)	Ro (μm)	AR (μm)	ρ (CN/μm^2)	$đ_o$ (μm)	$đ_e$ (μm)	R	VMR/DI
DZ	3,579	4,226,724.4	484,569.4	0.59	1.80	0.0084	202.04	17.18	11.76	182.17
CAZ	881	1,364,769	144,650.2	0.61	1.74	0.00064	272.02	20.00	13.60	310.17
DZ+CAZ	1,214	1,033,429	634.52	0.60	1.79	0.0011	148.43	14.58	10.18	78.80
DZ+MDZ	1,639	1,407,880.8	177,743.7	0.59	1.82	0.0011	148.42	14.65	10.13	88.94
DZ+CAZ+MDZ	1,242	1,555,484.6	177,395	0.59	1.82	0.00079	302.91	17.69	17.13	672.62
DZ+CAZ+MDZ+ERZ	743	1,009,806.8	97,770	0.59	1.82	0.00073	225.87	18.42	12.26	8.39

3.2 Cellular geometry: AR and roundness correlation for cellular appearance in the zones of *Fouquieria splendens* callus

Figure 3 shows the correlation between values of AR and roundness in cells of each *F. splendens* callus zones to make a detailed description of them if they are elongated or maintained the isodiametric form with a tendency of roundness. The average interval of cells first for the roundness values and after the AR values was as follows: DZ: 0.39 to 0.71 and 1.44 to 2.47μm; CAZ: 0.4 to 0.75 and 1.27 to 2.17μm; DZ+CAZ: 0.42 to 0.74 and 1.38 to 2.34 μm; DZ+MDZ: 0.39 to 0.72 and 1.36 to 2.33 μm; DZ+CAZ+MDZ: 0.37 to 0.72 and 1.37 to 2.37 μm and finally DZ+CAZ+MDZ+REZ: 0.4 to 0.77 and 1.4 to 2.32 μm. The global data (average values) for each zone is noted in Table 1. Finally, according to the roundness values that remained within a narrow range of 0.59 to 0.61, and the Aspect Ratio (AR) oscillated between 1.74 and 1.82 across all conditions; these results showed that cellular shape parameters revealed a strict geometric control within the *F. splendens* callus. It is of physiological interest that when evaluating the complex transitions involving the ERZ, this zone stabilized identically at 0.59 for roundness and 1.82 for AR. This mathematical consistency demonstrates that the interaction with the support of the remaining leaf tissue exerts a morpho-functional canalization pressure where cellular geometry is temporarily locked to prioritize the mechanical stability of the newly developing mass prior to the onset of massive volumetric expansion.

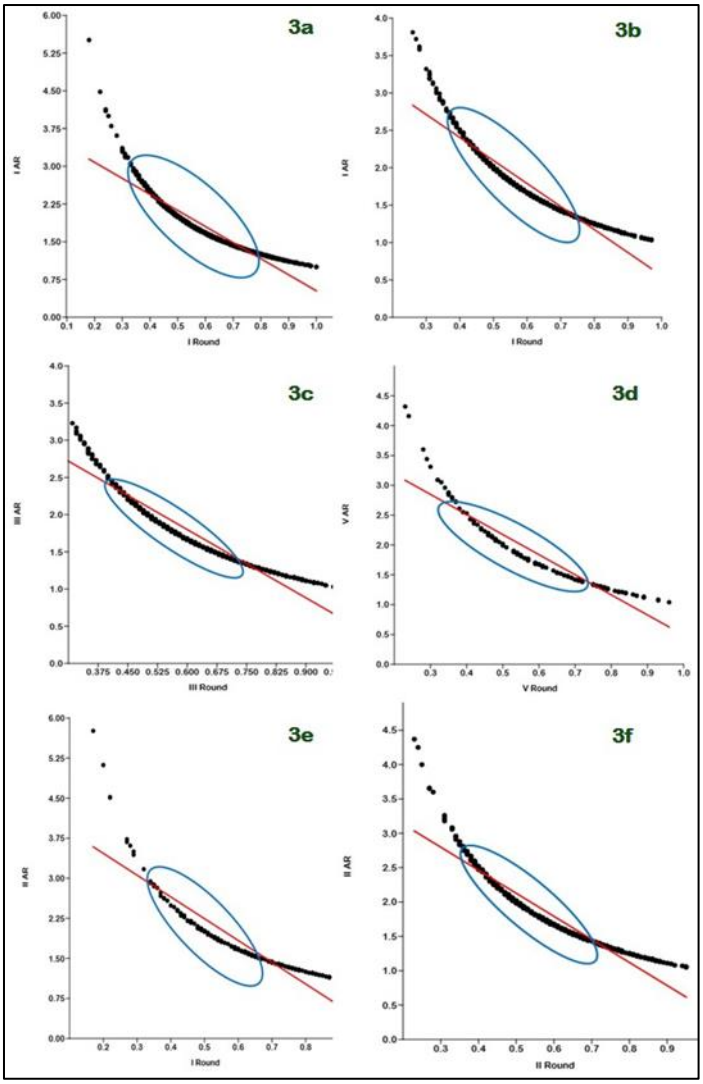

Figure 3 Representative linear regression curves showing the relationship between *Fouquieria splendens* callus aspect ratio (AR) and roundness: **3a)** DZ (r = 0.93); **3b)** CAZ (r =0.94); **3c)** DZ+CAZ (r = 0.94); **3d)** DZ+MDZ (r=0.92); **3e)** DZ+CAZ+MDZ (0.91) and **3f)** DZ+CAZ+MDZ+REZ (0.94). Groups of individual cells are shown in the plots.

Figure 4 shows the distribution arrangements of the cells of each callus zone, considering the centroid (x,y) data in a scatter plot representation, to see how the cells spread or aggregate and their cellular density and total area were considered for each zone. It is important to note that to achieve a rigorous and comprehensive characterization of cellular development, a dual spatial statistical framework was implemented by combining R Index and the VMR/DI index, all these data are noted in Table 1. The application of the R index was selected because it directly evaluates the physical distance. Its primary strength determines whether individual cells maintain a uniform, random, or clustered distance with respect to their nearest neighbors, providing a purely spatial closeness analysis. In complement, the VMR/DI index was employed to evaluate the counting homogeneity across the defined zones of *F. splendens* callus; the strength of this index is its capacity to determine whether the callus mass proliferates with equal intensity in all the zones analyzed, where the results of a variance equal to the mean denotes a completely homogeneous growth pattern; whereas an elevated variance reveals microstructural heterogeneity characterized by highly dense cellular "islands" coexisting alongside the zones. Therefore, integrating both descriptors was essential, allowing the simultaneous validation of micro-spatial cell regularity and macro-structural growth homogeneity throughout *F. splendens* callogenesis. The dual statistical approach utilizing the R index and VMR/DI index; revealed structural differences in the zones in *F. splendens* callus. All of them exhibited an R value greater than 1 (ranging from 10.13 to 17.13) mathematically demonstrating that individual cells maintain a hyper-regular dispersion pattern and constant spatial separation at the microcellular level, effectively preventing direct physical crowding. However, the macro-organization of the tissues showed sharp physiological variations associated with the biological origin of each zone when evaluating VMR values; where CAZ recorded an extremely elevated VMR (310.47) compared to the DZ (VMR = 182.17). From a

plant physiological perspective, this drastic increase in variance confirms that while CAZ cells microscopically repel each other to maintain vital cellular space, the global mass macroscopically organizes into hyper-dense "islands" or clusters, which are highly characteristic of active meristematic proliferation foci driving callogenesis.

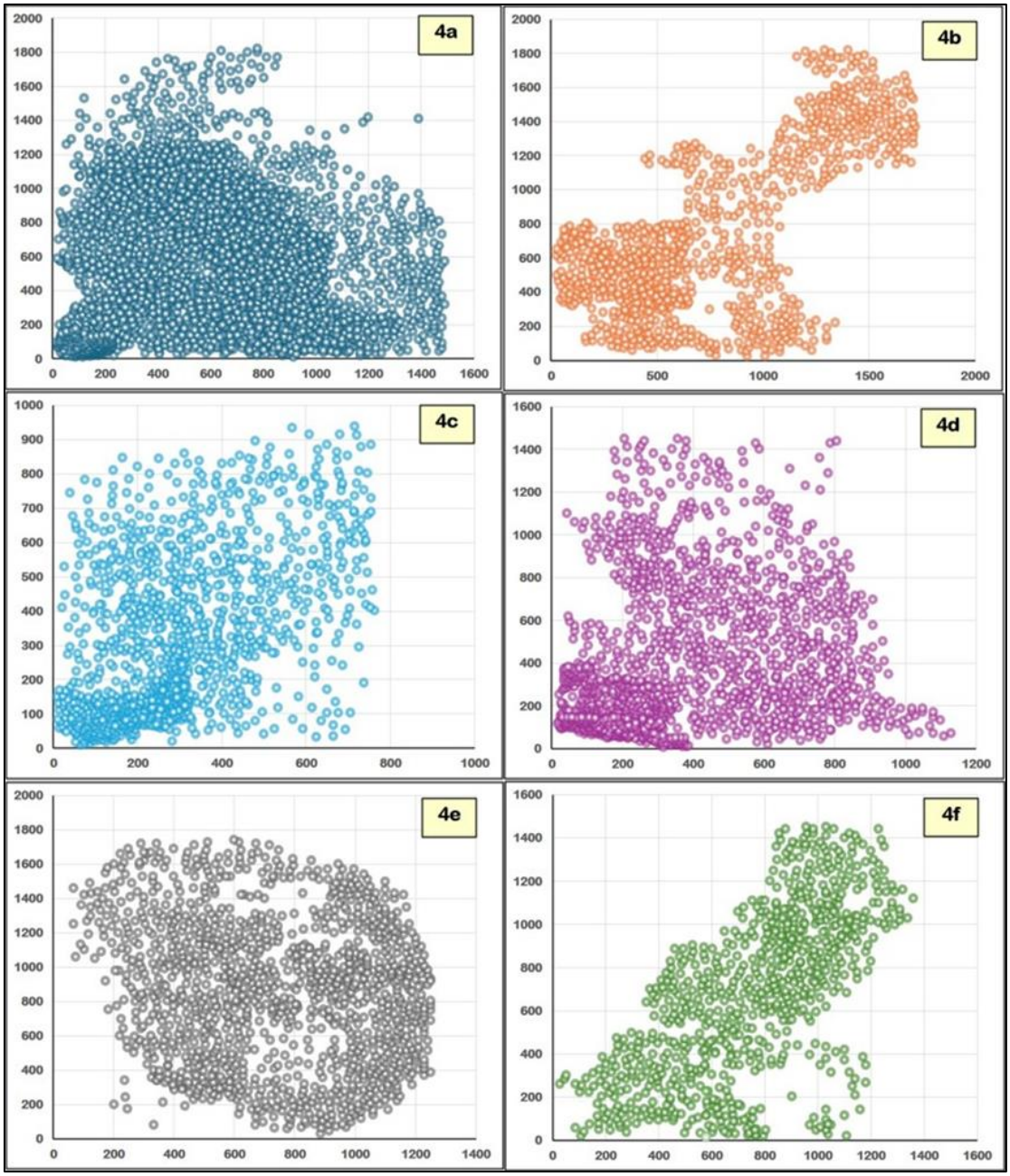

Figure 4 Scatter plot of cells distribution in the characterized zones of *Fouquieria splendens* callus: **4a)** DZ; **4b)** CAZ; **4c)** DZ+CAZ; **4d)** DZ+MDZ; **4e)** DZ+CAZ+MDZ and **4f)** DZ+CAZ+MDZ+REZ by centroid measurements.

When evaluating the combined zones; the interactions generated contrasting behaviors of high physiological interest. The “DZ+CAZ+MDZ” zone reached the highest dispersion index of the study (R = 17.13) accompanied by a maximum VMR/DI value (672.62). This phenomenon evidence maximum tissue heterogeneity where heavily populated zones simultaneously coexist with low-density areas while strictly preserving a coordinated microcellular geometry. Conversely, the “DZ+CAZ+MDZ+ERZ” zone caused a drastic drop in VMR/DI value to its lowest point (8.39), while maintaining an R index of 12.26. This transition toward a VMR/DI value close to theoretical homogeneity (VMR/DI→1) demonstrates an architectural stabilization of the callus; the ERZ acts as a regulatory structural support that evenly redistributes cell density across the plane, marking the maturation and homeostatic equilibrium of the developing *F. splendens* mass.

3.3 Principal Component Analysis (PCA) of cellular architectural variability: final zones characterization of the *Fouquieria splendens* callus

Figure 5 shows the PCA that successfully discriminated the developmental zones of *F. splendens* callus based on their morphometric and spatial attributes analyzed; capturing 73.34% of the total explained variance (PC1 = 42.30%; PC2 = 31.04%). The Biplot revealed a clear biological segregation, forming three major clusters defined by specific variable vectors. Principal Component 1 (PC1) was strongly and positively correlated with spatial and physical dispersion descriptors: DI, R, $đ_o$ and $đ_e$; this component distinctly isolates the "DZ+CAZ+MDZ" and the "CAZ". The projection of these treatments toward the right quadrant confirms that meristematic cluster formation and mechanical damage drive a critical increase in both micro-cellular regularity and macro-structural heterogeneity (high-density cell islands). Conversely, the "DZ+CAZ+MDZ+ERZ" zone clustered near the origin and inversely to the Ro vector, validating that the inclusion of explant remains buffers extreme variance and stabilizes tissue-plane homeostasis. Principal Component 2 (PC2) was dominated along its positive axis by large-scale cellular variables: CN, TA and TP. This axis completely segregated the "DZ"" into the upper quadrant, which physiologically denotes a mature tissue characterized by a high-volume fraction and expanded cellular biomass. In sharp contrast, the lower-left quadrant grouped "DZ+MDZ" and "DZ+CAZ", closely associated with the ρ and AR vectors. This evidences that early tissue combinations prioritize dense cellular packing and coordinated geometric elongation prior to the onset of macroscopical differentiation processes.

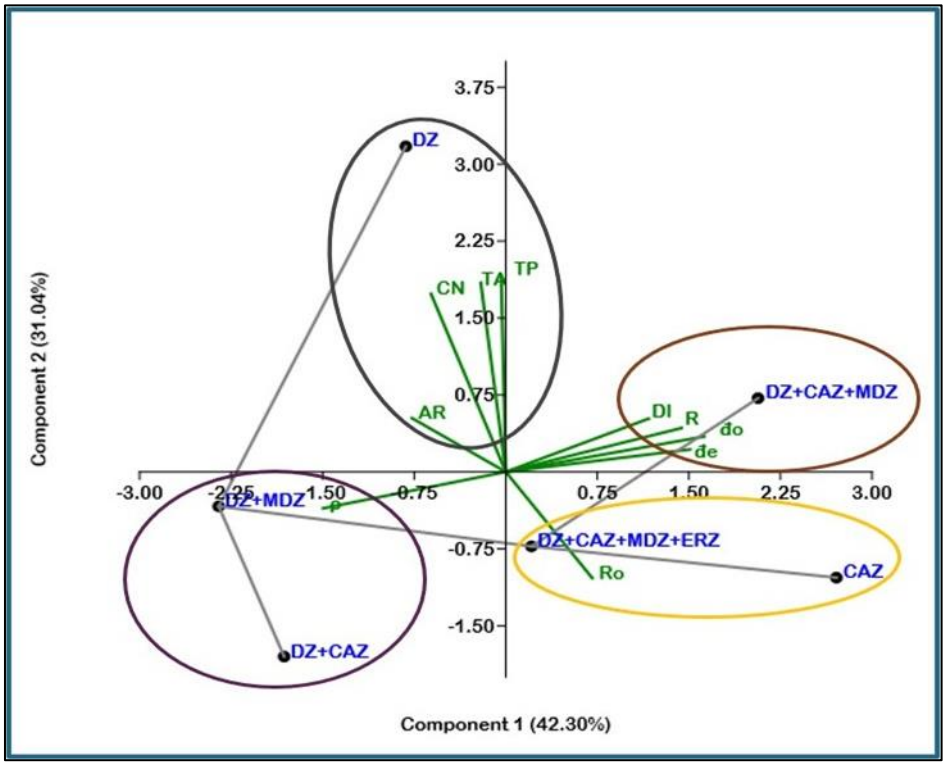

Figure 5 Principal Component Analysis (PCA) grouping the morphometric and cell spatial distribution in the determined zones of *Fouquieria splendens* callus.

In general, plant growth, development, and physiology are governed by complex processes across scales from molecular, cellular, tissue, and whole organism. Particularly, the plant *in vitro* studies have the attention on individual aspects of plant development: the specific role of hormones in regulating growth and/or the genetic control of cell differentiation [23,24]. Also, mathematical and computational analysis have emerged as powerful tools that allow the integration of experimental data associated to theoretical framework. Making this analysis together is possible to give mechanistic insights into multiple aspects of plant growth and development and predictions for the experimental search. Thus, the insight into plant growth, development, and physiology requires the employ of classical mathematical or computational concepts to understand the biological systems or processes [25]. Yunus et al. [26] suggest the image segmentation and post-processing of them are essential for the monitoring in tissue culture geometries description and become important strategies to the plant *in vitro* developmental research. In this work, the morphological changes of *F. splendens* callus analyzed by SEM images gives an initial approximation of its *in vitro* development, appearance and growth and how this interesting desert plant species begin to regenerate at 21 days.

4 Conclusion

The present study demonstrated the viability and high analytical value of implementing a robust, multivariate, and quantitative approach to characterize the cellular architecture of *Fouquieria splendens* callus. The Principal Component Analysis (PCA) successfully discriminated the developmental zones, accounting for 73.34% of the total explained variance and revealing that callogenesis is governed by discrete, predictable morphogenetic transitions. The Clark and Evans Index (R) consistently corroborated a coordinated and hyper-regular microcellular dispersion across all evaluated regions, effectively mitigating chaotic or disordered growth. Furthermore, the variance-to-mean ratio (VMR/DI) served as a highly sensitive macrostructural descriptor to map the wounding stress within the mechanical damage zones (MDZ) and meristematic cluster formation within the cellular aggregates zones (CAZ), additionally revealing that explant remains (ERZ) act as a homeostatic stabilizing agent that restores tissue density homogeneity. Finally, the fixed geometric canalization observed in roundness and aspect ratio parameters confirms that mechanical and structural stimuli strictly regulate cellular shape prior to massive volumetric cell expansion processes. Together, these mathematical descriptors lay the foundation for the automated monitoring, standardization, and optimal control of *in vitro* cellular mass development in xerophytic species of high ecological value.

Compliance with ethical standards

Acknowledgments

Authors are grateful to the Research Projects SIP-IPN: 20211499 and SIP-20221730, of the SPI-IPN, for providing the facilities to carry out this work and wish to thank for the fellowships from BEIFI- IPN; COFAA-IPN; EDI-IPN and SNI-CONAHCYT.

Disclosure of conflict of interest

The authors declare no conflict of interest.

References

[1] Abramoff MD, Magelhaes PJ, Ram SJ. Image processing with ImageJ. Biophotonics International. 2004; 11: 36-42.

[2] Collins TJ. ImageJ for microscopy. BioTechniques. 2007; 43: S25-S30.

[3] Olofsdotter M. Image processing: a non-destructive method for measuring growth in cell and tissue culture. Plant Cell Reports. 1993; 12:216-219.

[4] Uozumi N, Yoshino T, Shiotani S, Suehara K-I, Arai F, Fukuda T, Kobayashi T. Application of image analysis with neural network for plant somatic embryo culture. Journal of Fermentation and Bioengineering. 1993; 76:505-509.

[5] Smith M, Spomer LA, Meyer M, McClelland M. Non-invasive image analysis evaluation of growth during plant micropropagation. Plant Cell, Tissue and Organ Culture. 1989; 19:91-102.

[6] Smith MAL, Reid JF, Hansen AC, Li Z, Madhavi DL. Nondestructive machine vision analysis of pigment-producing cell cultures. Journal of Biotechnology. 1995; 40:1-11.

[7] Ibaraki Y, Kenji K. Application of image analysis to plant cell suspension cultures. Computers and Electronics in Agriculture. 2001; 30:193-203.

[8] Basu P, Pal A, Lynch J, Brown K. A novel image-analysis technique for kinematic study of growth and curvature. Plant Physiology. 2007; 145:305-316.

[9] French A, Ubeda-Tomas S, Holman TJ, Bennett MJ, Pridmore T. High-throughput quantification of root growth using a novel image-analysis tool. Plant Physiology. 2009; 150:1784-1795.

[10] Aitken-Christie J, Kozai T, Smith AL. Automation and environmental control in plant tissue culture. Springer, Berlin. 1994.

[11] Mora CF, Kwan AKH. Sphericity, shape factor, and convexity measurement of coarse aggregate for concrete using digital image processing. Cement and Concrete Research. 2000; 30:351-358.

[12] Hand C, Maki S, Reed BM. Modeling optimal mineral nutrition for hazelnut micropropagation. Plant Cell, Tissue and Organ Culture. 2014; 119:411-425.

[13] Honda H, Takikawa N, Noguchi H, Hanai T, Kobayashi T. Image analysis associated with a fuzzy neural network and estimation of shoot length of regenerated rice callus. Journal of Fermentation and Bioengineering. 1997; 84:342-347.

[14] Mansouri A, Fadavi A, Mortazavian SMM. Effects of length and position of hypocotyl explants on *Cuminum cyminum* L. callogensis by image processing analysis. Plant Cell, Tissue and Organ Culture. 2015; 121: 657-666.

[15] Skoog F, Miller CO. Chemical regulation of growth and organ formation in plant tissues cultured in vitro. Symposia of the Society for Experimental Biology. 1957; 11: 118-130.

[16] Chlyah H. Histological study of the formation of shoot and root meristems from internode segments of *Torenia fournieri* grown *in vitro*. Canadian Journal of Botany. 1974; 52: 473-476.

[17] Ikeuchi M, Favero DS, Sakamoto Y, Iwase A, Coleman D, Rymen B, Sugimoto K. Molecular mechanisms of plant regeneration. Annual Review of Plant Biology. 2019; 70: 377-406.

[18] Eshed-Williams L. Genetics of shoot meristem and shoot regeneration. Annual Review of Genetics. 2021; 55:661-81.

[19] Galeano J, Buceta J, Juarez K, Pumãri B, de la Torre J, Iriondo JM. Dynamical scaling analysis of plant callus growth. Europhysics Letters. 2003; 63:83-89.

[20] Murashige T, Skoog F. A revised medium for rapid growth and bioassays with tobacco tissues cultures. Physiologia Plantarum. 1962; 15: 473-497.

[21] Corona-Álvarez D, Salinas-Patiño VA, Hernández-Pimentel MV, Montes-Villafán S, García-Pineda M, Guerrero-Zúñiga LA, Rodríguez-Dorantes A. Morphological changes in *Fouquieria splendens* callus cocultivated with endophyte bacteria. International Journal of Current Microbiology and Applied Sciences. 2018; 7: 1577-1586.

[22] Clark PJ, Evans FJ. Distance to nearest neighbor as a measure of spatial relationships in populations. Ecology. 1954; 35: 445-453.

[23] Takatsuka H, Umeda M. Epigenetic control of cell division and cell differentiation in the root apex. Frontiers in Plant Science. 2015; 6:1178.

[24] Zhang Q, Gong M, Xu X, Li H, Deng W. Roles of auxin in the growth, development, and stress tolerance of horticultural plants. Cells. 2022; 11: 2761.

[25] Deb D, Chakrabortty B. Biophysical modelling as a tool for advancing plant science and engineering. Frontiers in Plant Science. 2025; 16:1693857.

[26] Egi Y, Oter T, Hajyzadeh M, Catak M. Real-time callus instance segmentation in plant tissue culture using successive generations of YOLO architectures. Plants. 2026; 15: 47.